Surface Science 97 (1980) 25–42

PROTEIN DEPOSITION ON FIELD-EMITTER TIPS AND ITS REMOVAL BY UV RADIATION *

J.A. PANITZ
Sandia National Laboratories †, Albuquerque, New Mexico 87185, USA

and

I. GIAEVER
General Electric Research and Develoment Center, Schenectady, New York 12301, USA

Received 14 January 1980

Protein deposition on field-emitter tips has been examined using Transmission Electron Microscopy to view the protein coated tip profile. A single layer of adsorbed protein is barely if at all detectable, but double and triple layers produced by the immunologic reaction can be directly observed. As a result, the thickness and morphology of antigen–antibody layers has been directly observed for the first time. Tips exposed first to Bovine Serum Albumin (BSA) and then to anti-BSA rabbit serum are covered with a reasonably uniform, double protein layer ≈130 Å thick. This layer can be built-up to a triple layer ≈275 Å thick by additional exposure to anti-rabbit IgG goat serum. Surface tension forces during the drying process which follows protein deposition appear to affect the thickness and morphology of the protein layers. The oxidation and subsequent change in the morphology of a protein layer exposed to ultraviolet radiation has also been observed using TEM. The destruction of a triple protein layer at a rate of ≈0.5 Å/s is observed for tungsten tips exposed to ≈6 W of UV radiation from a high-pressure mercury arc in laboratory ambient. These results are compared to those obtained from a simple, visual test for protein layer adsorption in which submonolayer coverages of protein can be detected with the unaided eye.

1. Introduction

During the development of a new microscopy to image macromolecular contours [1,2] we have found it necessary to investigate the deposition of protein onto, and its removal from, the apex of tungsten field-emitter "tips". These tips, prepared by electropolishing polycrystalline tungsten wire or rod [3], are field-evaporated [4] or thermally annealed in high vacuum to obtain a smooth, hemi-

* This work was supported by the US Department of Energy under Contract DE-ACO4-76-DP00789.
† A US Department of Energy Facility.

spherical apex, 800–5000 Å in radius. Previous procedures which employed freeze-drying to place molecules on the tip apex [5], electrophoretic attachment of the molecules to the tip surface [6], or touching the tip apex with a molecule coated metallic plate [7], could be evaluated only in terms of their ability to produce molecular images in the Field-Electron-Emission Microscope [3] or Field-Ion Microscope [3]. Unfortunately, the images which were obtained did not display convincing molecular contours, so that information regarding individual deposition procedures was at best, highly subjective.

In the present work we will examine protein deposition in two ways: (1) using a simple technique in which the presence of submonolayer quantities of protein can be visually determined by the unaided eye [10,11], and (2) using a high resolution Transmission-Electron Microscope (TEM) [8] to directly image protein layers deposited on tungsten field-emitters. Because TEM image contrast is poor for unstained protein molecules in monolayer or submonolayer coverage, we will use the immunologic reaction [9] to build-up double and triple layers which are easily observed. The uniformity of these layers will be used to compare two aqueous deposition procedures, and to evaluate the role of surface tension in the deposition process.

Because it is time-consuming to prepare and characterize individual field-emitter tips, it is desirable to re-use a tip for several protein deposition experiments. With this goal in mind, we have also investigated the removal of protein layers from field-emitter tips that were exposed in laboratory ambient to UV radiation from a high-pressure mercury arc.

2. Emitter tip preparation

Two different field-emitter configurations were used in this study which, for convenience, we will designate as type 1 and type 2 field-emitters. Type 1 field-emitters were prepared for electropolishing by spot-welding a short length of 0.15 mm diameter, polycrystalline tungsten wire to a 1.5 mm diameter, type 304 stainless-steel support rod, 16 mm in length. A portion of the rod was ground flat to facilitate spot-welding. Type 2 field-emitters were prepared for electropolishing by grinding a 5 mm length of 1.5 mm diameter, polycrystalline tungsten rod 16 mm in length, to a diameter of 0.4 mm. Fig. 1 shows both types of field-emitters following electrochemical polishing to a fine point in ≈1.6M KOH using a standard thin-layer polishing technique [12]. The type 2 field-emitter is particularly useful for TEM imaging experiments because it cannot be magnetized. (Although the type 1 field-emitter is made from materials which are initially nonmagnetic, the spot-welding process locally magnetizes the 304 stainless-steel support rod.)

After electrochemical polishing, the sharp field-emitter tips were placed in an ultra-high vacuum environment. Each tip was then field-evaporated [4] at cryogenic temperatures to form an atomically smooth, hemispherical apex 200–500 Å in

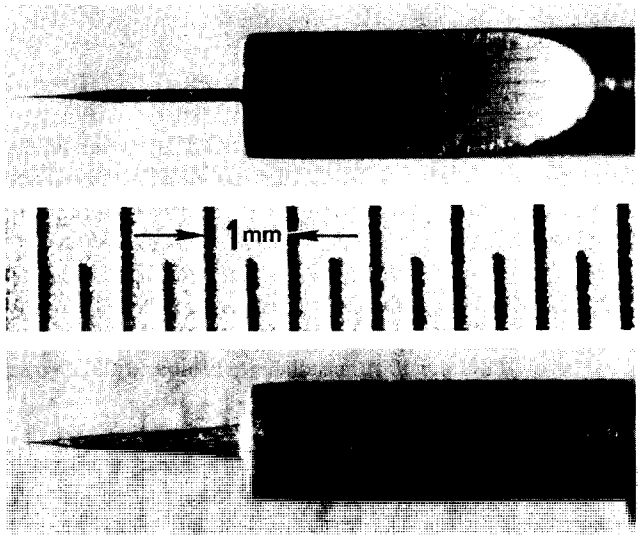

Fig. 1. Upper: A "type 1" field emitter prepared by electrochemical polishing of a polycrystalline tungsten wire, spot-welded to a flattened, type 304 stainless-steel support rod. Lower: A "type 2" field-emitter prepared by electrochemical polishing of a polycrystalline tungsten rod, ground to a 0.4 mm diameter over a portion of its length to facilitate electropolishing.

radius, or thermally annealed by electron-bombardment to form a smooth (but thermally faceted) hemispherical apex 500–5000 Å in radius. As a result of these procedures we could prepare clean, smooth, field-emitter tips over a wide range of radii, allowing us to qualitatively examine the role of emitter radius in the protein deposition process.

3. Protein deposition

In this paper we will restrict our discussion to a very simple protein deposition procedure – immersion of a field-emitter tip into a solution of the protein at room temperature. The adsorption of protein on the tip apex will then be limited by the diffusion of protein molecules to the tip, and depend only on the concentration of the solution, and the time of immersion. Since protein molecules are very large compared to any other species in solution, they will be the only adsorbed species capable of being observed in the electron microscope. However, in order to image the protein coated tips in the electron microscope, they must be moved through a liquid/air interface, dried, and placed in a high-vacuum environment. We have found that surface tension forces during the drying process will affect the uniformity of

the protein layers. (In principle, surface tension forces could be eliminated by employing the well-established critical point drying technique [13]).

To define the parameters of concentration and immersion time prior to tip deposition, we have used a simple technique in which the adsorption of submonolayer quantities of protein can be visually observed with the unaided eye. The technique, developed previously by one of us to study the antibody–antigen reaction [10,11], employs a specially prepared substrate that consists of a thin glass slide coated with isolated indium particles in the 1000 Å size range. A typical slide transmits ≈70% of the light incident upon it, and appears golden-brown in color due to light scattered from the indium particles.

If a slide is immersed in a protein solution, the rate of protein adsorption on the slide will depend mainly on the protein concentration and the degree to which the solution is stirred. The optical density of the slide will change with time until a time-independent density is achieved. At this point a monolayer coverage of protein will have been reached. If the slide is removed from the protein solution before this time, washed with distilled water, and blown dry with compressed (oil free) air or nitrogen, its optical density will be a measure of the degree of protein coverage. Although the optical density of the slide will not increase linearly with protein coverage, a qualitative estimate of protein coverage can be made by comparing the optical density of the slide following protein adsorption to the maximum optical density corresponding to a coverage of one monolayer.

Surprisingly large changes in optical density are observed for small changes in protein adsorption on the slide. This effect is primarily due to the large increase in the resonance scattering of incident electromagnetic radiation from the small, conducting indium particles as they become coated with a dielectric layer [14] of protein. Because the effect is so large, the adsorption of even a fraction of a monolayer of protein can be easily observed with the unaided eye. Furthermore, since the indium particles are approximately spherical with an average radius of 1000 Å, they are a good approximation to the size and shape of the field-emitter apexes used in this study. Although indium and tunsten surfaces may bind protein differently, we have observed little difference in the thickness of a protein layer estimated from the change in optical density of an indium slide, and from a direct measurement of the thickness of a protein layer observed on a tungsten field-emitter in the TEM.

For this study three protein solutions will be used: (1) a solution of bovine serum albumin (BSA), (2) a solution of anti-BSA rabbit serum containg BSA-specific antibodies, Ab_1, of the IgG type and (3) a solution of anti-rabbit IgG goat serum containing Ab_1-specific antibodies, Ab_2. Since thick protein layers display sufficient contrast for imaging in the TEM, we form them by first adsorbing a monolayer of BSA on the tip surface. We then rinse the tip in distilled water (to remove any species not tightly bound to its surface), and then expose the monolayer of BSA to the anti-BSA rabbit serum. Because of the immunologic reaction, the antibody molecules in the serum will attach themselves specifically to the adsorbed BSA to form a second layer. After rinsing again in distilled water a triple

layer can be produced, in this case by exposing the antibody molecules in the second layer to a solution of anti-rabbit IgG goat serum. Each stage in the formation of these multiple protein layers can be followed by observing the change in optical density of an indium slide exposed to the same proteins under identical dosing conditions.

The slides have proven to be very useful in the field-emitter tip studies because they permit predefining deposition conditions under which protein is most likely to adsorb. By using the slides, one avoids time-consuming TEM observations of emitters which are not coated with protein as would occur (for example) if the protein was unknowingly supplied in phosphate or borate buffers. These buffers will prevent the adsorption of protein on a surface [15] – a fact known to the detergent industry and demonstrated by the slides, but easily overlooked.

Once optimum dosing conditions have been determined by use of the slides, one of two immersion methods are used to deposit protein onto the field emitter apex. The first, or "droplet method", involves placing isolated drops ($\approx$0.05 cm^3) of BSA, rabbit serum containing Ab_1, goat serum containing Ab_2, and distilled water onto the surface of a clean teflon block. (Four shallow, circular depressions drilled into the block surface conveniently define and separate each of the four droplets.) The field-emitter tip is carefully lowered into the BSA droplet for the required deposition time. It is then raised out of the droplet and lowered into a droplet of distilled water for several seconds to rinse the emitter tip of any poorly adhering species. After raising the tip out the distilled water droplet, the dipping procedure is repeated for each of the other proteins, with a fresh droplet of distilled water used for each successive rinse.

The second immersion method – the "bucket-method" – was designed to minimize the numerous traversals of a liquid/air interface inherent in the droplet method. The procedure is shown schematically in fig. 2. One (or several) emitter tips are placed into predrilled holes in a small teflon holder, or "bucket". The bucket is then lowered into a small beaker containing sufficient BSA ($\approx$1 cm^3) to completely cover the apexes of the emitter tips when it is fully immersed in the protein solution. After remaining in BSA for the required time period, the entire beaker of BSA is immersed into a much larger beaker containing approximately 400 cm^3 of distilled "rinse" water. Without breaking the water/air interface, the teflon bucket is extracted from the small beaker with tweezers, and placed alongside of it on the bottom of the large beaker. The smaller beaker (which now contains only diluted BSA) is removed from the larger beaker, washed in distilled water, and lowered back into the large beaker. The teflon bucket is then reinserted into the small beaker with tweezers, again without breaking the water/air interface. If the small beaker is now removed from the larger beaker, the teflon bucket and tips will be totally immersed in a solution of BSA diluted with distilled water by the ratio of the volume of the large-to-small beaker (i.e. 400 : 1). In practice, this rinsing process is usually repeated at least one more time to insure a BSA dilution (or rinse) of $(400)^2$: 1 or approximately, 10^5 : 1. At this point the tips have experienced only

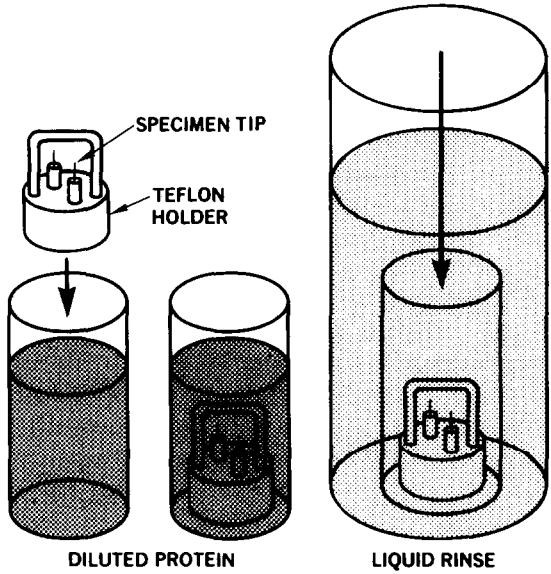

Fig. 2. The "bucket-method" of depositing protein onto field-emitter tips as described in the text. This procedure has the advantage of minimizing the number of traversals of liquid/air interfaces experienced by a tip during multi-layer protein deposition (i.e. surface tension effects are minimized).

one traversal through a liquid/air interface – the interface encountered during initial insertion into BSA. If the final rinse is performed with physiological saline (0.154N) instead of distilled water, the next protein can be added directly to the small beaker. For example, rabbit serum containing Ab_1 added to the small beaker will be diluted by the saline already in the beaker to the desired concentration for Ab_1 dosing.

The process is then repeated for each additional protein so that after removing the bucket from the final rinse solution, the tips will have experienced only two traversals of a liquid/air interface – during initial immersion into BSA, and during removal from the final rinse solution.

Since a slide can be immersed into each protein solution with the teflon bucket (and rinsed with the bucket), one can verify that the predetermined dosing parameters have been correctly established.

4. TEM imaging procedure

After protein is deposited onto a field-emitter tip, the tip is inserted into an adapter which is placed into a TEM specimen holder [16] (fig. 3A). The specimen

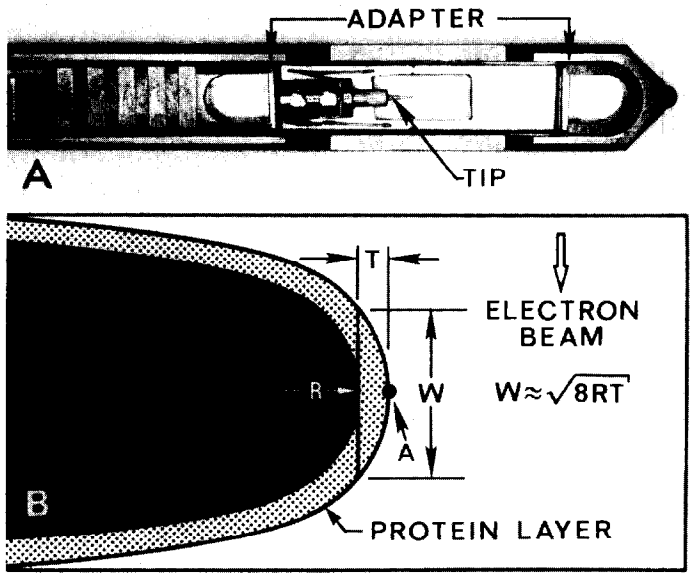

Fig. 3. (A) "type 2" field-emitter tip retained in an adapter which is held in a JEOL, SCSH specimen holder; the specimen holder is inserted into the TEM equipped with a side-entry goniometer stage for imaging. (B) A schematic view of a hemispherical field-emitter tip of apex radius, R, on which a protein layer of uniform thickness, T, has been deposited; W is the maximum thickness of protein traversed by the primary electron beam during TEM imaging (see text).

holder is then inserted into the TEM [8], equipped with a side-entry goniometer stage. During TEM imaging, a shadow of the protein coated tip profile is projected onto a photographic emulsion with a magnification of approximately 10^5. The field-emitter tip appears black in the TEM image because electrons cannot penetrate through it to expose the photographic emulsion. On the other hand, adsorbed protein appears as a shade of grey in the TEM image because it scatters electrons less effectively than the emitter tip, thereby allowing some electrons to penetrate and partially expose the photographic emulsion. The number of electrons which reach the emulsion (and determine the density of the protein image) will depend on the amount of adsorbed protein traversed by the electron beam. Even for a uniformly thick layer of protein, the amount of protein traversed by the electron beam is not constant, but is a function of the beam position relative to the emitter tip surface. This effect is schematically shown in fig. 3B where the maximum distance, W, traversed by the electron beam in the protein layer is given as a function of the emitter tip radius, R, and the thickness, T, of the uniform protein layer. Consequently, a TEM image of a uniform protein layer should vary in density from a maximum at the emitter tip surface, to a minimum at the outer edge of the layer

(point A in fig. 3B). In practice, such a change in image density is often observed, but only for $W \gtrsim 1500$ Å. The edge of the protein layer is usually well defined in the TEM image because the TEM is focussed on the layer boundary – point A in fig. 3B. Ocassionally, it is difficult to focus the TEM image, or the image will be seen to drift within the field of view. We attribute these effects to charging by the electron beam. Such difficulties seem to be more prevailant when thick protein layers (≈150 Å) are imaged, but are fortunately an uncommon occurrence [17].

5. TEM imaging

When BSA is deposited onto the surface of an indium slide, the optical density of the slide will increase (corresponding to an increase in the coverage of BSA on each indium particle). If Ab_1 is now applied, the density of the slide will again increase, and if Ab_2 is deposited on top of the BSA–Ab_1 layer, a further increase in optical density will be observed. However, since the Ab_1 antibody binds specifically to BSA (and Ab_2 does not) a BSA coated slide exposed first to Ab_2 and then to Ab_1 will not increase in optical density. Similarly, a field-emitter tip exposed to BSA–Ab_1 will become coated with a protein layer which is visible in the TEM image (fig. 4A), while a tip exposed to BSA–Ab_1–Ab_2 will be coated with a thicker layer (fig. 4C). However, a tip exposed to BSA–Ab_2–Ab_1 will show no layer build-up. This demonstrates that the immunologic reaction occurs in vitro on a tungsten field-emitter tip whose surface can be directly imaged in the TEM. In the sense that the slide technique accurately predicts the course of protein deposition on the field-emitter tips, the two techniques can be said to yield consistent results. It should be noted that although we are able to observe a BSA monolayer on an indium slide, we cannot observe a BSA monolayer on a field-emitter tip in the TEM. We believe the maximum distance traversed by the electron beam in penetrating such a layer is too small to permit adequate image contrast.

Since the TEM images will allow us to follow an immunologic reaction by directly observing the thickness of antibody layers, it is important to ask how quantitative are thickness measurements made in this way. Although there has been disagreement in the literature regarding the minimum thickness of BSA and Ab_1 layers [18–20], recent ellipsometry measurements place the minimum thickness of a combined BSA + Ab_1 layer at ≈80 Å [21], assuming that the index of refraction of protein is 1.55. (The thickness of the layer is very sensitive to this assumption since an index of refraction of 1.50 will increase the layer thickness by ≈30%.) Strictly speaking, ellipsometer measurements cannot distinguish between a uniform or nonuniform layer – the ellipsometer really only measures the amount of material per unit area. Thus we may regard the ellipsometer result as a minimum thickness. On the other hand, the maximum thickness cannot exceed the combined molecular sizes ≈200 Å. In fig. 4 we show the results of an experiment where the protein has been deposited by the "droplet" method onto type 1 tungsten field-

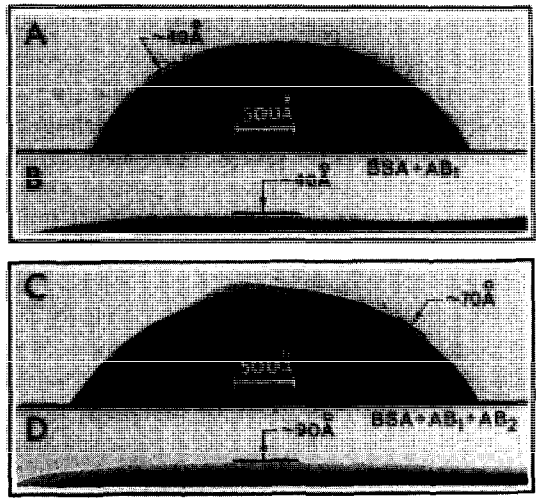

Fig. 4. (A) A thermally annealed, "type 1", tungsten field-emitter tip dosed with BSA and a single antibody layer, Ab_1 by the "droplet-method" (see text); 100 μg/ml of BSA for 120 s/rinse/undiluted anti-BSA rabbit serum for 300 s/rinse; all protein dilutions and rinses performed with distilled water; the BSA + Ab_1 layer is too thin (GE Micrograph 318 LIA). (B) A view of a region of the same tip along its shank; the BSA + Ab_1 layer in this region is also too thin (GE Micrograph 318 LIA). (C) Another thermally annealed, type 1, tungsten field-emitter tip dosed with BSA and two antibody layers, Ab_1 and Ab_2 by the "droplet-method" (see text); 100 μg/ml of BSA for 120 s/rinse/undiluted anti-BSA rabbit serum for 300 s/rinse undiluted anti-rabbit IgG goat serum for 300 s/rinse; all protein dilutions and rinses were performed with distilled water; the BSA + Ab_1 + Ab_2 layer is too thin (GE Micrograph 318 HIA). (D) A view of a region of the same tip along its shank; the BSA + Ab_1 + Ab_2 layer is too thin (GE Micrograph 318 HIA).

emitters. From the electron micrograph of fig. 4A we find that the average BSA + Ab_1 layer thickness is ≈40 Å, measured near the tip apex where the curvature of the emitter is large. In fig. 4B we find that the average layer thickness measured along the tip shank (where the curvature is less pronounced) is also 40 Å. Since 40 Å is about one-half of the minimum BSA–Ab_1 layer thickness, we must conclude that we are observing an artifact – an anomalously thin protein double layer. This conclusion is reinforced by observing the thickness of a BSA + Ab_1 + Ab_2 layer deposited on field-emitter tips. For example, in fig. 4C, the average thickness of such a layer near the tip apex is ≈70 Å. This is greater than the thickness measured for the BSA + Ab_1 layer (as it should be), but again much too small since it is also less than the minimum thickness expected for the BSA + Ab_1 layer alone. However, the thickness of the BSA + Ab_1 + Ab_2 layer measured along the shank of the tip (fig. 4D) is greater (≈90 Å), and the layer in this region of the emitter appears more uniform. In general, we always observe a more uniform layer of more

reasonable thickness in regions of the emitter which are less sharply curved than the apex. We also find that a more uniform layer of protein is deposited on large radius emitter tips ($R \approx 2500$ Å) than on tips with smaller radii ($R \approx 500$ Å). These observations hold true for tips made of tungsten and molybdenum and despite a more limited number of trials, seem to apply also to tips made of gold. In other words, the thickness and uniformity of protein layers deposited onto field-emitter tips appears to be at least reasonably independent of tip material, but dependent on the curvature of the tip surface. It is known that the surface tension of water can exert extremely large compressional stresses on structures having a high curvature when such structures traverse a liquid/air interface during drying [13]. Qualitatively, the compressional stress on a molecule during the drying process is equal to γ/r where $\gamma \approx 70$ dyn/cm is the surface tension of water and r is the molecular radius [13]. For protein molecules this is of the order of 10^8 dyn/cm^2. If the drying process is not symmetric with respect to the molecule a shear force will also be present which can move the adsorbed molecule over the tip surface. Because of the small radius of curvature of the tip apex, water will evaporate faster from the apex of the tip than from the shank. This occurs because the vapor pressure of a liquid increases with increasing surface curvature [22]. As a result, an evaporating layer of water will move towards the tip apex during drying, and the resulting asymmetry in the force caused by surface tension will cause some adsorbed molecules to move toward the tip apex. This explanation is consistent with our observations that protein layers tend to be more nonuniform at the tip apex, that the nonuniformity becomes more pronounced as the layer thickness increases, and that layer inhomogenity seems to be less pronounced with tips of larger radii. If surface tension forces are responsible for causing the anomalies which we observe in fig. 4, we should obtain more reasonable results by minimizing the number of traversals of the tip through a liquid/air interface during dosing. This was accomplished by developing the "bucket-dosing" procedure of fig. 2 in which only one liquid/air traversal of importance is encountered (during the removal of the tip from the final rinse liquid). A typical result for a type 2 field-emitter on which BSA + Ab_1 was deposited is shown in fig. 5B, and in fig. 7 (at $t = 0$) for BSA + Ab_1 + Ab_2. In fig. 5B the BSA + Ab_1 layer is quite uniform and has a reasonable thickness (≈130 Å), while the BSA + Ab_1 + Ab_2 layer of fig. 7 also has a reasonable thickness (≈275 Å). The fact that neither layer if perfectly uniform in thickness suggests that surface tension forces may still be active in determining layer morphology, even though these forces have been minimized by the dosing method. It would be instructive to eliminate surface tension forces entirely, by eliminating even a single traversal through a liquid/air interface. Perhaps this can be accomplished by employing the critical point drying procedure used by electron microscopists to overcome surface tension difficulties [13].

We made a further interesting observation during the initial use of the bucket-dosing procedure. When type 1 field-emitters were used (tungsten wire spot-welded to a 304 stainless-steel support rod), we observed that BSA + Ab_1 layers were often anomalously thick. Fig. 5A shows one example of a BSA + Ab_1 layer on a type 1

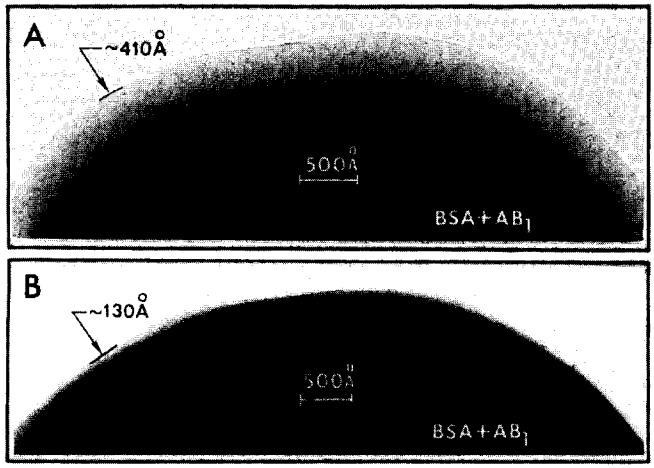

Fig. 5. (A) A thermally annealed, type 1, tungsten field-emitter tip dosed with BSA and a single antibody layer, Ab_1 by the "bucket-method" (see text); 100 μg/ml of BSA for 120 min/rinse/1 : 10 dilution of anti-BSA rabbit serum for 30 min; all protein dilutions and rinses performed with 0.154N saline; the layer thickness is anomalously high due to an electrochemical reaction between the tungsten tip wire and a stainless-steel support (see text) (GE Micrograph 318 VIA). (B) A thermally annealed, type 2, tungsten field-emitter tip dosed with BSA and a single antibody layer, Ab_1 by the "bucket-method" (see text); 250 μg/ml of BSA for 300 s/rinse/1 : 10 dilution of anti-BSA rabbit serum for 30 min; all protein dilutions and rinses performed with 0.154N saline with 0.01M Tris at pH 7.5; the layer thickness is "correct" (see text) (GE Micrograph 520 AIA).

field-emitter using the bucket-dosing procedure. The average layer thickness is seen to be ≈410 Å, anomalously high. A possible explanation is that the dissimilar materials of the type 1 field-emitter (tungsten and 304 stainless-steel) may react electrochemically when immersed in the dosing solutions. To examine this possibility, we constructed a test cell using 1 cm^2 tungsten and stainless-steel plates separated by 1 mm. When the gap between the plates was filled with distilled water, an instantaneous emf of 90 mV was measured (across a 1 MΩ input to an oscilloscope). This emf decreased over ≈30 s to a steady-state value of ≈60 mV. With 0.154N saline solution placed between the plates, an instantaneous emf of ≈60 mV was measured, which decreased to a steady-state value of ≈50 mV. In both cases the tungsten plate was the cathode. Although we could not observe a protein precipitate at the tungsten electrode when shorted to the stainless steel electrode (with BSA placed between the plates), we did observe a precipitate in a similar cell using indium and gold electrodes. In this case a protein precipitate formed at the indium electrode, probably because trivalent indium ions which are released into solution acted as chelating centers for charged protein molecules in solution. For the tung-

sten–stainless-steel cell the electrochemistry is much more complex, but it is clearly desirable to eliminate electrochemical reactions of any type. For this reason we fabricated the type 2 (solid tungsten) field-emitters described previously. Type 2 field-emitter tips, used in conjunction with the bucket-dosing procedure, always produced the most uniform protein layers of most reasonable thickness.

6. Protein removal

Indium slides and tungsten field-emitter tips were coated with protein and exposed to UV radiation in laboratory air. A Hanovia type SH high-pressure mercury arc lamp [23] was selected for the UV source because of its previous use in this application [24]. The lamp produces approximately 6.25 W of UV radiation between 0.22 and 0.37 μm and $\approx$7.5 W of visible and infrared radiation. Without substrate cooling, substrate temperatures as high as 400°C can be reached during protein desorption experiments. To insure that the indium slides retain their integrity and the tungsten tips are not thermally oxidized, we kept the substrate at $\approx$40°C. Although the removal of protein from metal surfaces under UV radiation in air has not been discussed in the literature, several investigations [24,25] have indicated that other organic contaminants are removed by such a treatment. For example, the cleanliness of two gold surfaces contaminated with lubricating oil was monitored as a function of UV exposure by measuring the coefficient of adhesion between the surfaces brought into contact [26]. In this section we will extend and quantify these previous results by using indium slides and the TEM to observe the UV cleaning process more directly.

Indium slides and field-emitter tips were placed approximately 3 cm below the UV lamp on an air-cooled platform whose temperature could be monitored. A 600 cc pyrex beaker (wrapped in aluminum foil to eliminate the glare from the operating arc) was placed over the lamp, slides and/or tips, to prevent free air circulation in their vicinity. To observe the cleaning process as a function of time, we first prepared an indium slide by coating one-third of the slide with BSA, and one-third with BSA + Ab_1. The remaining third of the slide was not coated with protein. The slide, covered with an opaque piece of paper, was placed under the operating UV lamp. The beaker was then placed over the lamp and slide in such a way as to allow a portion of the paper covering the slide to protrude under its rim. By moving the paper, narrow regions of the slide could be successively exposed to the UV radiation. This process is shown schematically in the upper portion of fig. 6. The lower portion of fig. 6 shows a photograph of an actual slide exposed in this manner, with UV exposure time increasing from right-to-left. To re-iterate, the top third of the slide was exposed to BSA + Ab_1, and the middle third to BSA only. The bottom third of the slide was not exposed to protein. At $t = 0$ (corresponding to no UV exposure), the BSA + Ab_1 double layer density is observed to be about twice the density of the BSA monolayer. In turn, the BSA monolayer is observed to have

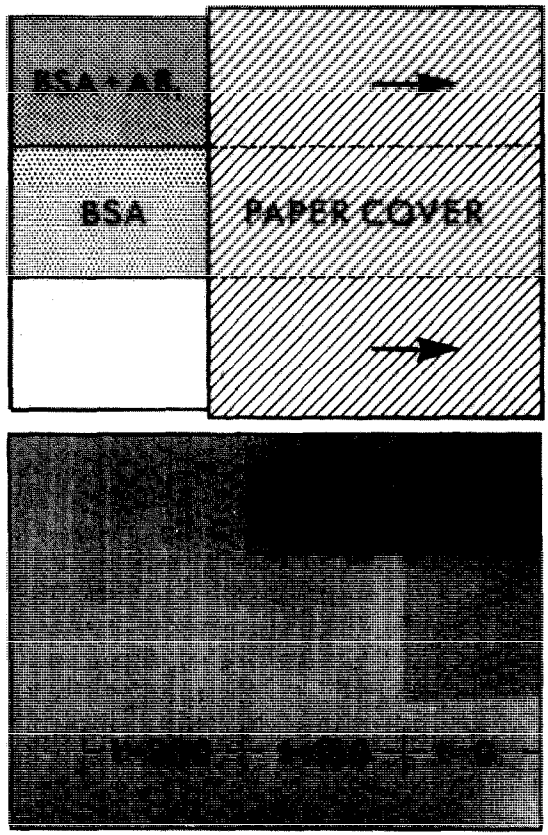

Fig. 6. Upper: A schematic drawing of how the surface of an indium slide dosed with BSA and BSA + Ab_1 is exposed to a UV source (see text). Lower: A photograph of an indium slide showing the effect of UV exposure on BSA and BSA + Ab_1 layers as a function of exposure time, t (see text).

about twice the density of the protein free portion of the slide. At $t = 150$ s, the density of the BSA + Ab_1 layer has decreased to about half of its value at $t = 0$ and appears to be about equal to the density of the unexposed BSA monolayer at $t = 0$. From this change in density we can cautiously conclude that 150 s of UV exposure has removed about one-half of the BSA + Ab_1 layer. On the other hand, after 150 s of UV exposure, the BSA layer density appears to be equal to that of the protein-free slide. This implies that 150 s of UV exposure removes the BSA monolayer completely. After 300 s of UV exposure, the BSA + Ab_1 layer density has almost decreased to that of the protein free slide. (The unaided eye can observe that the layer has not been completely removed from the slide although the photograph of

the slide cannot record the small change in contrast corresponding to the amount of BSA + Ab_1 remaining.) Finally, after 450 s of UV exposure, the optical density of the BSA + Ab_1 layer has decreased to that of the protein free slide. These observations imply that $\gtrsim$300 s of UV exposure is required to remove a BSA + Ab_1 layer from small, indium particles.

To observe the UV cleaning phenomena more directly, TEM micrographs were used to record the removal of protein layers from tungsten field-emitter tips as a function of UV exposure time. Prior to UV exposure a protein coated tip was imaged in the TEM to record the initial protein layer thickness and morphology ($t = 0$). Then, after each of a series of 150 s UV exposures, the tip was again transferred to the TEM for imaging. Because of consistencies in the series of TEM images which we obtained, we concluded that the protein layer thickness and morphology was not affected by exposure to laboratory air during tip transfer between the UV source and the TEM.

The TEM images of BSA + Ab_1 layers exposed to UV radiation confirmed the removal time for the complete layer ($\approx$300 s) observed with the indium slides. In fig. 7 we show a series of micrographs for a thicker protein layer of BSA + Ab_1 + Ab_2 exposed to UV radiation. After 450 s of UV exposure, a noticeable amount of the layer remains on the tungsten surface. (This is confirmed by indium slide observations when a slide is covered with BSA + Ab_1 + Ab_2.) After 600 s, some protein residue is still observed over the tip surface. The thicker region of protein at the right-hand side of the tip apex (visible at $t = 0$ as a noticeable, nonuniformity in the thickness of the smooth protein layer) has been markedly attacked by the UV process. After 750 s of UV exposiure this region has been further attacked, and a close examination of the tungsten tip profile also reveals subtle changes in the morphology of the originally smooth tungsten surface. We attribute these localized changes in surface morphology to the formation of tungsten oxide inclusions caused by the extended UV exposure in air. Ellipsometry measurements on an evaporated tungsten film deposited on a glass substrate support this hypothesis. They show a layer build-up of $\approx$30 Å following UV exposure for 750 s in air.

From fig. 7 a qualitative protein removal rate of $\approx$0.5 Å/s can be extracted by determining the time required to completely remove the 275 Å thick portion of the original layer at $t = 0$. Since the intensity of the UV radiation at the position of the tip (or slide) was not measured, this rate can only serve as an indication of how rapidly this particular UV source removes thick protein layers – at a substrate temperature of $\approx$40°C.

The mechanism responsible for protein removal by UV radiation is not known in detail, but must involve UV formation of an active oxygen species since the rate of cleaning depends on oxygen partial pressure [24]. This effect can be easily observed with an indium slide. If laboratory air is allowed to circulate freely over a slide during UV exposure, the rate of protein removal is markedly decreased. Since the temperature of the slide is kept constant, this can only be attributed to the continuous removal of an active oxygen species – probably ozone – from the surface

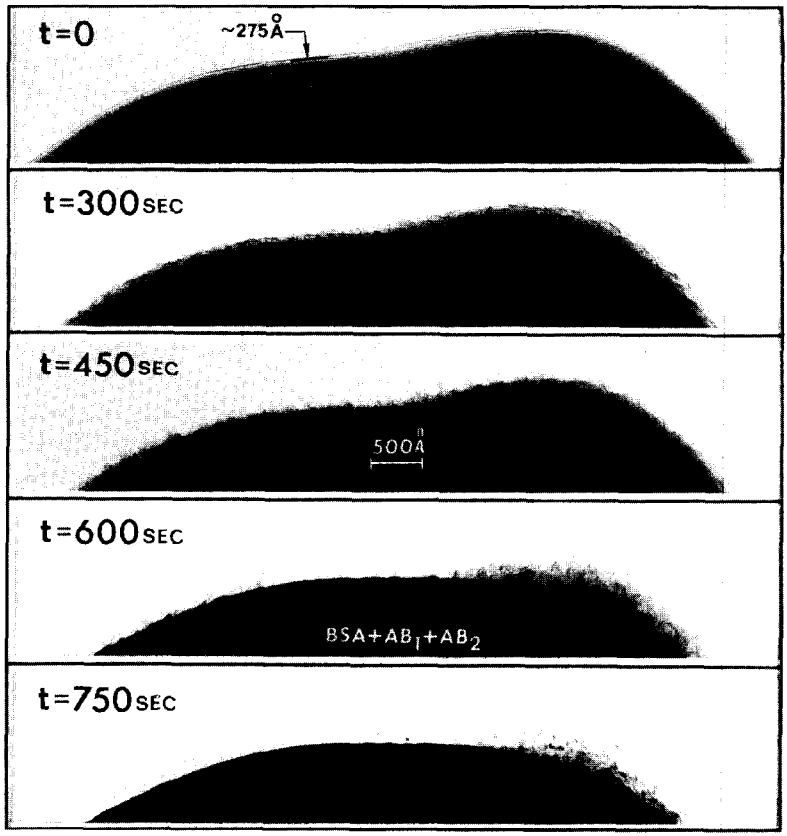

Fig. 7. A thermally annealed, type 2, tungsten field-emitter as a function of exposure to 6.25 W of UV radiation from a high pressure mercury arc in laboratory air. The tip was dosed with BSA and two antibody layers, Ab_1 and Ab_2 using the "bucket-method" (see text). 250 μg/ml of BSA for 300 s/rinse/1 : 10 dilution of anti-BSA rabbit serum for 30 min/rinse/1 : 10 dilution of anti-rabbit IgC goat serum for 30 min. The BSA was diluted in 0.154N saline, the serums were diluted in 0.154N saline + 0.01M Tris, pH 7.5. The average layer thickness at $t = 0$ (no UV exposure) is "correct" (see text) (GE Micrographs 520 CIA, 520 GIA, 520 I1A, 520 KIA, 520 MIA).

of the slide. In order to demonstrate that direct UV irradiation of the protein layer is also important, we placed a glass plate several millimeters above a portion of a protein covered slide. The glass plate prevented direct UV irradiation of the protein layer beneath it, but allowed active oxygen species to interact with the surface of the slide. Once again, the rate of protein removal was markedly decreased. The implication is that UV photons must interact directly with the protein layer in order for the cleaning process to occur rapidly. We speculate that UV photons have sufficient energy to break chemical bonds within the protein layer, thereby allowing

protein residues to be oxidized by free oxygen and ozone. (Such a process is probably responsible for the characteristic "mottled" appearance of the layer seen in fig. 7 after prolonged UV exposure.) Even carbonaceous residues, normally difficult to remove, will eventually be converted into CO and CO_2 which can rapidly diffuse into the gas phase. The trick is to establish conditions of UV exposure and substrate temperature such that the protein is completely removed without appreciably oxidizing the underlying substrate.

7. Summary and conclusions

The immunologic reaction has been used to produce thick protein layers on field-emitter tips. Layer thickness and morphology have been studied by transmission electron microscopy. By minimizing surface tension forces encountered during aqueous dosing, and by eliminating electrochemical reactions during protein deposition, uniform protein layers of reasonable thickness have been obtained. In general, it appears easiest to deposit uniformly thick protein layers on field-emitter tips having a smooth, hemispherical apex of large radius (>1500 Å).

The antigen–antibody reaction resulting from exposure of a BSA-coated tip to anti-BSA rabbit serum results in a BSA–antibody layer ≈130 Å thick. This is consistent with layer thicknesses between 80 and 200 Å, estimated from more indirect evidence. By exposing a BSA coated tip to anti-BSA rabbit serum and then to anti-rabbit IgG goat serum, a triple protein layer is produced by the immunologic reaction. The average thickness of this layer measured from TEM micrographs is ≈275 Å. Since reasonably uniform, thick protein layers can be deposited on field-emitter tips by dosing from aqueous solution, we conclude that submonolayer coverages of isolated protein molecules can also be achieved by the proper choice of dosing parameters. However, forces induced by surface tension during tip drying (following aqueous protein deposition) may change the distribution of molecules on the emitter tip apex, or distort an individual molecule's morphology. For this reason, a critical-point-drying procedure [13] may be desirable.

The removal of protein layers from field-emitter tips under UV irradiation in laboratory air has also been studied. We find for double antibody layers that the rate of protein removal is ≈0.5 Å/s when 6.25 W of UV radiation from a high pressure mercury arc is used. Since we did not measure the UV intensity at the tip during exposure, this result is qualitative, but consistent with the rate of protein removal determined from an indium slide technique discussed in the text. Our measurements also confirm previous speculations that both UV radiation and an active oxygen species (probably ozone) are required to produce the UV cleaning effect. TEM micrographs have shown that the cleaning process effectively removes all of the protein deposited on a tungsten field-emitter tip (to within the resolution of the TEM ≈5 Å), although a slight change in the morphology of the tungsten surface can be noticed after long UV exposures.

Acknowledgements

The authors wish to thank Mr. E.D. Koch of the General Electric Research and Development Center who provided TEM support for this work, and Mr. G.L. Fowler of Sandia National Laboratories who developed the techniques required to make "type 2" field-emitters, and assisted in all technical aspects of this investigation.

References

[1] Abstracts of papers presented at the 25th Intern. Field-Emission Symposium, The University of New Mexico, Albuquerque, New Mexico, 1978, in: Ultramicroscopy 4/3 (1979) 361.
[2] Abstracts of the 39th Annual Physical Electronics Conference, The University of Maryland, College Park, Maryland, 1979.
[3] E.W. Müller and T.T. Tsong, Field-Ion Microscopy: Principles and Applications (Elsevier, Amsterdam, 1969) p. 119.
[4] Ref. [3] p. 56.
[5] R.C. Abbott, Rev. Sci. Instr. 36 (1965) 1233.
[6] Ref. [3] p. 290.
[7] Ref. [3] p. 292.
[8] JEOL JSEM-200 Scanning Transmission Electron Microscope.
[9] F.A. Ward, A Primer of Immunology (Butterworth, London, 1970).
[10] I. Giaever, J. Immunology 110 (1973) 1424.
[11] I. Giaever, J. Immunology 116 (1976) 766.
[12] Ref. [3] p. 119.
[13] H.P. Burstyne and A.A. Bartlett, Am. J. Phys. 43/5 (1975) 414.
[14] H. Scharfman, J. Appl. Phys. 25 (1954) 1352.
[15] H.T. Trurnit, Science 111 (1950) 1.
[16] JEOL SCSH Common Specimen Holder.
[17] Focussing difficults, and problems with image drift are observed more frequently in the JEOL JSEM-100 Scanning Transmission Electron Microscope. Charging of the protein layer may be a function of the incident beam energy, so that the effect would be more noticeable in this 100 kV machine than in the 200 kV machine which we usually use (ref. [8]).
[18] L. Vroman and A.L. Adams, Surface Sci. 16 (1969) 438.
[19] A. Rothen and C. Mathot, Helv. Chim. Acta 54 (1971) 1208.
[20] C.A. Fenstermaker, W.H. Grant, B.H. Grant, B.W. Morrissey, L.E. Smith and R.R. Stromberg, NBSIR 74-470, March 22, 1974 (The National Bureau of Standards, Washington, DC).
[21] R.W. Deblois, The General Electric Research and Development Center, Schenectady, NY, private communication.
[22] The fractional change in vapor pressure, P/P_0, can be determined from the Kelvin equation $RT \ln P/P_0 = 2\gamma V/r$, where V is the molecular volume ($\approx 3 \times 10^{-23}$ cm^3 for water). At 300 K, for a tip radius $r = 100$ Å, the vapor pressure at the tip surface $P \approx 1.11\ P_0$, where P_0 is the normal vapor pressure of water. See, for example, A.W. Adamson, Physical Chemistry of Surfaces (Interscience, New York, 1960) p. 56.

[23] Canrad Precision Industries, Inc., Hanovia Lamp Division, 100 Chestnut St., Newark, NJ 07105.
[24] R.R. Sowell, R.E. Cuthrell, D.M. Mattox and R.D. Bland, J. Vacuum Sci. Technol. 11/1 (1974) 474.
[25] D.A. Bolon and C.O. Kunz, Polymer Sci. Eng. 12 (1972) 109.
[26] R.E. Cuthrell and D.W. Tippling, Rev. Sci. Instr. 47/5 (1976) 595.